DNMI DET NORSKE METEOROLOGISKE INSTITUTT

klima

THE DESIGN REFERENCE YEAR

ARVID SKARTVEIT, HANS LUND
AND JAN ASLE OLSETH

REPORT NO. 11/94 KLIMA

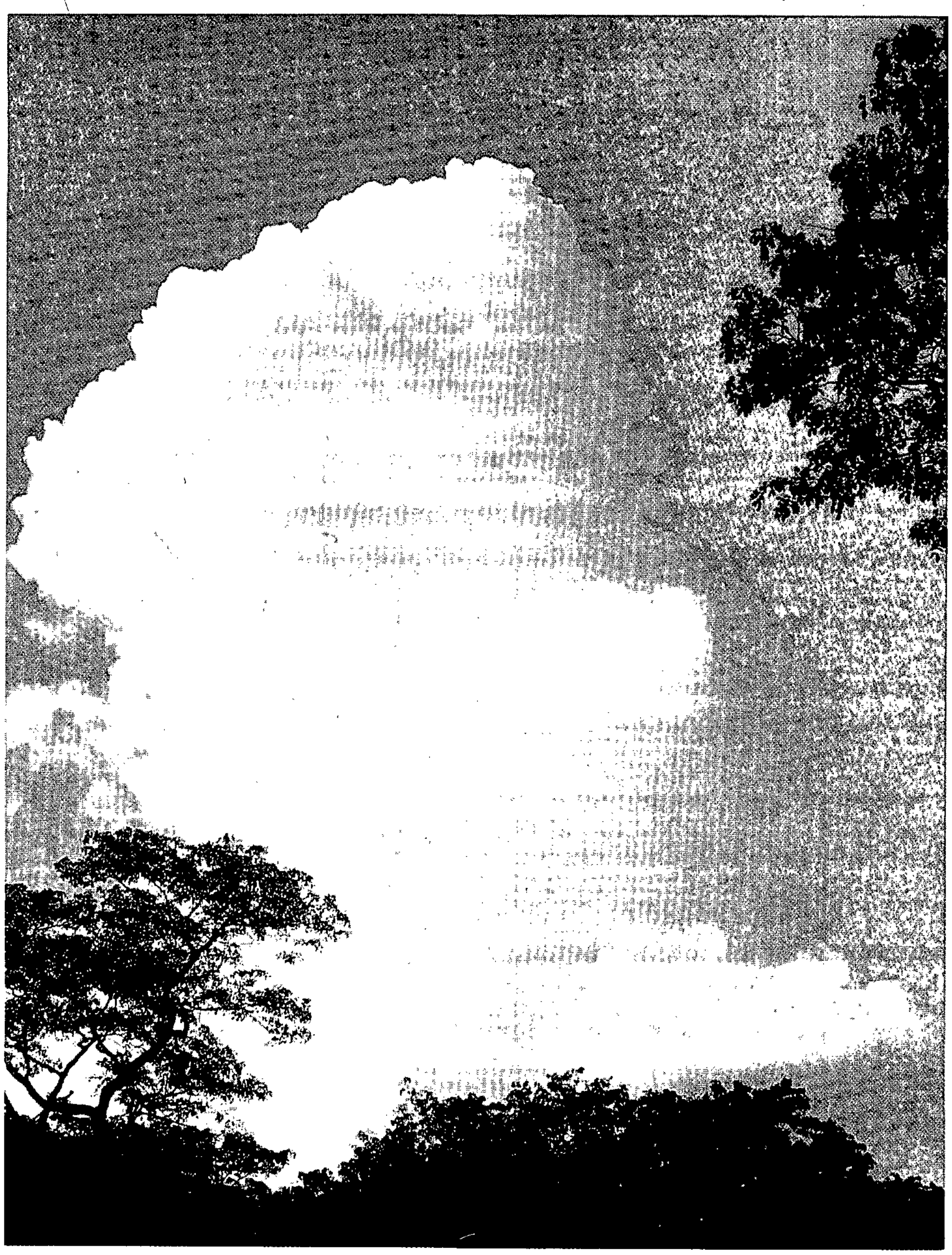

DNMI-RAPPORT

THE NORWEGIAN METEOROLOGICAL INSTITUTE
P.O. BOX 43 BLINDERN 0313 OSLO 3

PHONE: (02) 96 30 00

ISBN

REPORT NO.
11/94 KLIMA

DATE
12.04.1994

TITLE

THE DESIGN REFERENCE YEAR

AUTHORS

ARVID SKARTVEIT, Geophysical Institute, Univ. of Bergen
HANS LUND, Technical University of Denmark
JAN ASLE OLSETH, The Norwegian Meteorological Institute

PROJECT CONTRACTOR

International Energy Agency, Solar Heating and Cooling Programme
The Norwegian Meteorological Institute

SUMMARY

A Design Reference Year (DRY) consist of 8760 concurrent hourly weather parameters for one location. Its main use as input to computer simulations of building and solar energy system performance, require that its parameters are representative with respect to frequency distributions and auto-/crosscorrelation structure. A few examples of observed distributions and correlation structures are given.

Since it is difficult to produce "synthetic" DRYs that fulfil the above requirements, DRYs are often made by linking together selected months or seasons, or selecting entire years from data observed in the past. The three steps in the production of a "Semi-synthetic" DRY are outlined: a) Select for each calendar month the best month from a multi-year record; b) Adjust the best month to the multi-year distribution for important weather parameters; c) Reconstruct unavailable data from existing data.

The paper is based on a presentation at the seminar: Recent Advancements in Solar Radiation Resource Assessment in Denver, Colorado, USA, November 16-19, 1992.

SIGNATURE

Jan Asle Olseth — Bjørn Aune

Jan A. Olseth, Senior Scientist — Bjørn Aune, Head of Climatology Division

CONTENTS

1. INTRODUCTION

The evaluation of solar energy systems, building energy consumption, energy conservation, indoor climate and comfort, is not done by using long-term averages of weather data as input, but preferentially by using some generated collection of weather data representative of the climatological features of the site in question [1]. A Design Reference Year (DRY) [2] is a such collection of weather data for one year, arranged as 8760 hourly sets of simultaneous weather parameters. A DRY is valid for a limited geographical area only, and for most countries several DRYs are needed to cover the entire area.

The Design Reference Years can be seen as a new generation of data collections already known as Test Reference Years (TRY) [3,4,5] or Typical Meteorological Years (TMY) [6,7,8,9]. Compared to existing TRYs the DRYs have some new parameters and more representative averages and standard deviations for many parameters.

DRYs are used as input data for computer simulations, which can be done either for a single project to be evaluated against standards or building codes, or for comparison of two or more projects, e.g. by cost-benefit analyses. The former purpose will place the most exacting demands on the DRY data.

The present work describes parts of the work made in connection with the IEA Solar Heating and Cooling Programme, task 9, Subtask E: "Representative Design Years for Solar Energy Applications". The participants in this subtask have been: R. Festa and C.F. Ratto, University of Genova, J.A. Olseth, The Norwegian Meteorological Institute/University of Bergen, A. Skartveit, University of Bergen, B. Aune, The Norwegian Meteorological Institute, L. Dahlgren, Swedish Meteorological and Hydrological Institute, T.W. Püntener and K. Mathis, EMPA, Zürich, and H. Lund (coordinator), Technical University of Denmark. Further valuable contributions have been delivered by E. Maxwell, NREL (SERI), R. Perez, State University of New York, F. Kasten and G. Czeplak, MOH, German Weather Service, and other participants in the task 9 work. The Subtask E participants produce DRYs for their own countries, and a "Design Reference Years Producers Manual" and a "Design Reference Years Users Manual" is in preparation.

2. REQUIREMENTS FOR DESIGN REFERENCE YEARS

Most applications of a DRY require that the most important of its weather parameters are representative with respect to:

i) Frequency distributions.
ii) Autocorrelation structure.
iii) Crosscorrelation structure.

2.1. The frequency distributions

Since most systems respond non-linearly to weather parameters, these should have not only representative averages, but also representative frequency distributions in a DRY.

Although long-term averages of most weather parameters tend to be normally, or at least unimodally distributed, many of them deviate significantly from the normal distribution in the case of hourly and even daily averages.

For example, over extensive regions of the Earth, cloudiness shows a characteristic frequency distribution with the extremes as the most frequent values (modes). This U-shaped cloud cover frequency distribution, exemplified for Bergen and Ås at about 60°N in Norway (Fig. 1, [10]), is "mapped" into the irradiation domain in a way that augments the number of "poor" and "excel-lent" hours/days of sunshine at the expense of "average" hours/days. This bimodal distribution pattern reflects the "on-off" character of solar irradiance, and it varies with the monthly average as shown for hourly and daily global clearness index in Fig. 2 [10,11]. The bimodality significantly affects non-linear radiation-driven processes, and it should therefore be adequately reflected in a DRY.

2.2 The autocorrelation structure

In addition to non-linear responses, most buildings and solar systems possess an inertia or a "memory". This makes their response to e.g. solar radiation dependent even on the succession in which the hourly irradiances occur. Also weather has a "memory", over a spectrum of time scales, which yields a positive autocorrelation for most weather parameters.

For example, based on data from the U.S, Switzerland and Sweden [12,13], the lag one auto-correlation coefficients for normalized global clearness index (global irradiation : cloudless

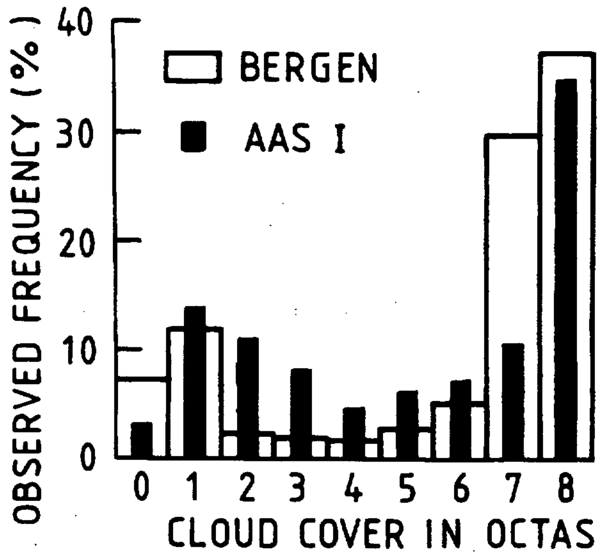

Fig.1 Cloud cover frequency distribution at Bergen (1965-79) and Ås (1968-79) at 60°N Norway, based on observations at 7, 13 and 19 CET [10].

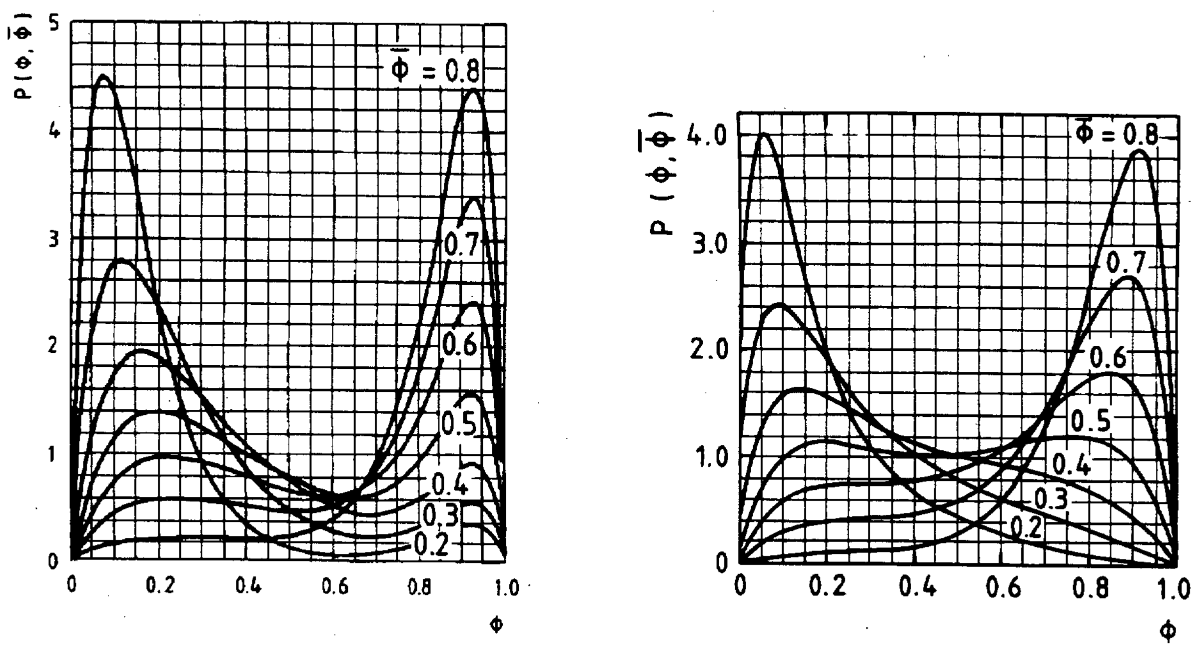

Fig.2 The probability density function P of hourly (left) and daily (right) normalized clearness index ϕ (global irradiation : maximum global irradiation) [10,11].

irradiation) were 0.92 - 0.94 (5 min), 0.86 - 0.88 (hours), and 0.36 - 0.41 (days). Rather than occurring at random, sunny or cloudy weather thus occur in spells having a duration distribution which in general varies with location and season. One effect of this persistency is demonstrated in Fig. 3 for Bergen and Ås [14,15]. For example, increasing the averaging time from 1 to 10 days narrows the 10 - 90 percentile range of June global radiation by approximately a factor 2. If the days occurred in random sequence, a narrowing by approximately a factor 3 ($10^{1/2}$) would be expected.

2.3 The crosscorrelation structure

In addition to being non-linear and dependent on past values, a system's response to any single weather parameter in general depends also on the simultaneous and past values of other weather parameters. For example, the cooling effect of air depends on both temperature and wind, and the efficiency of a liquid heating collector depends on irradiance, temperature and wind. Realistic crosscorrelations between weather parameters are therefore important qualifications of a DRY.

Fig. 4 exemplifies the crosscorrelation between air temperature and global radiation at Bergen and Ås [15]. A causal relation and the thermal inertia of the climatic system, yields a positive correlation between calendar month averages of global radiation and air temperature, with the global radiation preceding the air temperature by approximately one month. Moreover, reflecting both different distances from the western coast and screening effects of a mountain range between the two stations, the curve through the pairs of monthly averages changes from the station on the western coast (Bergen) to the station more inland (Ås). The correlation between daily air temperature and global radiation ranges from about -0.5 in mid-winter to about 0.5 in mid-summer. This mainly reflects that summer clouds at this latitude (60°N) tend to reduce solar heating more than they increase greenhouse warming, while the opposite tends to be true for winter clouds. The negative winter crosscorrelation is most pronounced at the coastal station. This is due to the fact that the mid-latitude winter contrast, between mild cloudy oceanic air and cold dry continental air, is most strongly felt right at the western coast. Finally, and not shown here, a causal relation again yield a positive correlation between hourly global radiation and air temperature, with the global radiation preceding the air temperature by a couple of hours.

The general lesson exemplified in Fig. 4, is that the crosscorrelation structure of meteorological data derives from a multiplicity of factors. It therefore varies with site, season and time scale in a complex way.

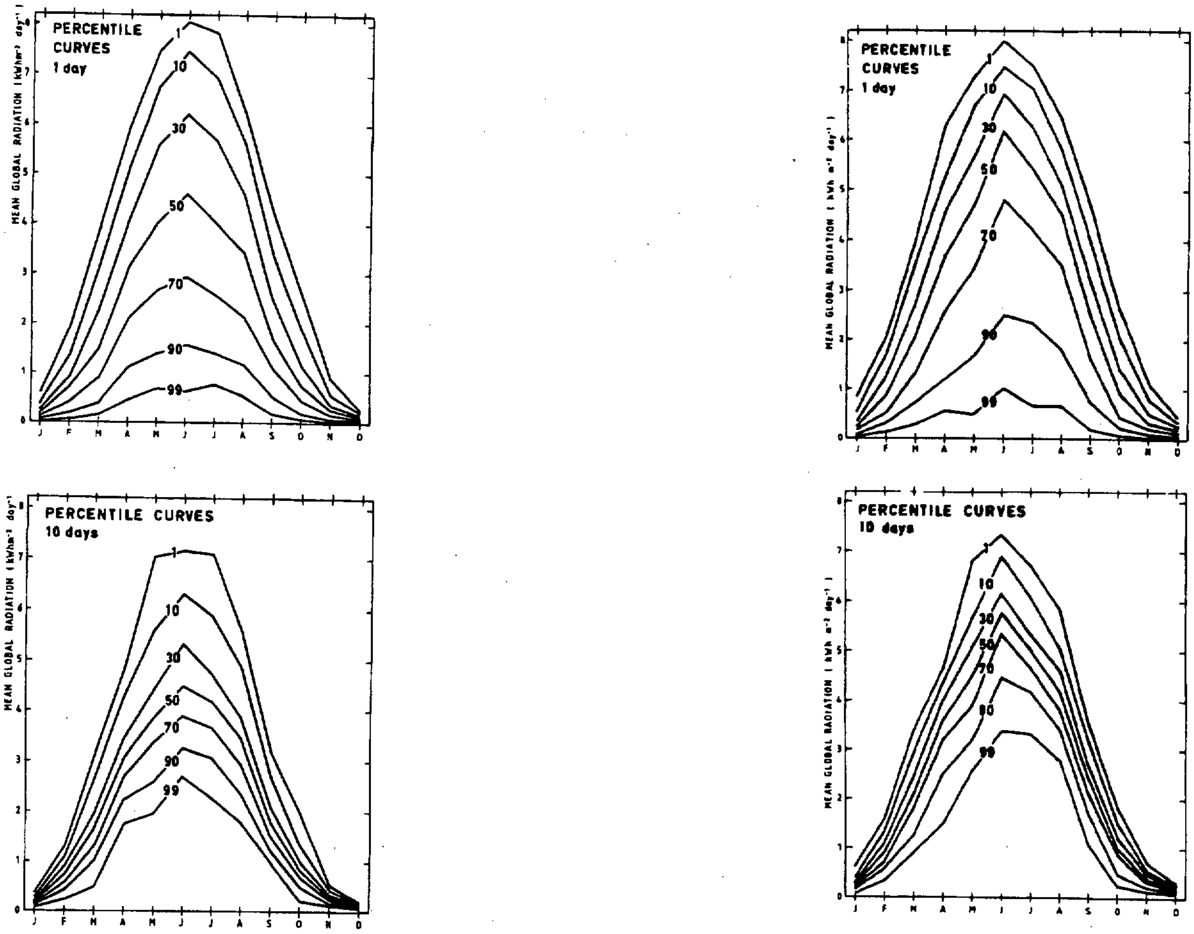

Fig.3 Percentile curves of daily and ten days global irradiation at Bergen (left) and Ås (right) [14,15].

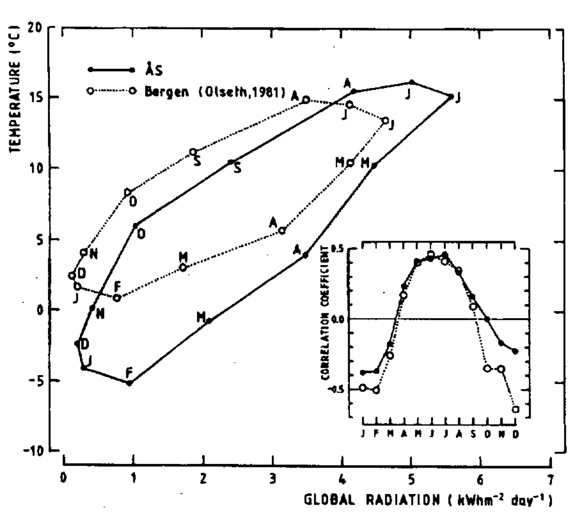

Fig.4 Left: Calendar month averages (12 years) of air temperature vs. global radiation at Bergen and Ås. Right: Monthly correlation coefficients between daily air temperature and global radiation [15].

3. PRODUCTION OF DESIGN REFERENCE YEARS

Due to the complex auto- and crosscorrelation structure of meteorological data, it is difficult to produce "synthetic" DRYs from climatic averages, that fulfil all the above requirements i)-iii). "Non-synthetic" DRYs are therefore often made by linking together selected months or seasons, or even selecting entire years from data observed in the past.

The production of a "semi-synthetic" DRY has three steps:

a) A selection process: For each of the twelve calendar months the "best" month is selected from, preferably, more than 10 years of data.

b) An adjustment process: The "best" month is given the long-term frequency distribution for important weather parameters.

c) A reconstruction process: Unavailable parameters are derived from existing data.

3.1 The selection process

The output from a computer simulation with a DRY as input, should deviate as little as possible from the output obtained by using the complete multi-year meteorological record as input. Since DRYs are used for a variety of simulations, it follows that the selection of the "best" month can not be strictly unambiguous. Several adequate selection methods therefore exist [6,16,17,18].

Considering the most common applications of DRYs, daily average and maximum air temperature (dry bulb) and daily global radiation are judged to be the most important weather parameters. The "Danish" selection method [3] therefore searches, as outlined below, the multi-year record for the "best" months having the "most typical" means and variations for these three parameters. For the mid-winter months at high latitudes, sunshine duration is preferred instead of global radiation for this search process.

For each weather parameter p, daily residuals r_p are first calculated for each date d, month m, and year y:

$$r_p(d,m,y) = p(d,m,y) - F_p(d,m) \quad , \tag{1}$$

where the smoothed multi-year average $F_p(d,m)$ is generated from harmonic analysis of the multi-year record of daily values $p(d,m,y)$. Monthly means and standard deviations of these daily residuals are then formed (NM = number of days in the month):

$$r_p(m,y) = \frac{\sum_{d=1}^{NM} r_p(d,m,y)}{NM} \quad , \tag{2a}$$

$$\sigma_p(m,y) = \left\{ \frac{\sum_{d=1}^{NM} \left[r_p(d,m,y) - r_p(m,y) \right]^2}{(NM - 1)} \right\}^{0.5} \quad . \tag{2b}$$

For each of the 12 calendar months, averages and standard deviations of these monthly r_p and σ_p are now formed over the NY years in the record:

$$r_p(m) = \frac{\sum_{y=1}^{NY} r_p(m,y)}{NY} \quad , \tag{3a}$$

$$\sigma_p(m) = \frac{\sum_{y=1}^{NY} \sigma_p(m,y)}{NY} \quad , \tag{3b}$$

$$\sigma_{rp}(m) = \left\{ \frac{\sum_{y=1}^{NY} \left[r_p(m,y) - r_p(m) \right]^2}{(NY - 1)} \right\}^{0.5} \quad , \tag{3c}$$

$$\sigma_{\sigma p}(m) = \left\{ \frac{\sum_{y=1}^{NY} \left[\sigma_p(m,y) - \sigma_p(m) \right]^2}{(NY - 1)} \right\}^{0.5} \quad . \tag{3d}$$

Note that the multi-year average residuals $r_p(m)$ are close to zero. The following dimensionless numbers quantify how the individual monthly averages (2a) and standard deviations (2b) deviate from the corresponding calendar month averages (3a-b):

$$D_{rp}(m,y) = \frac{r_p(m,y) - r_p(m)}{\sigma_{rp}(m)} \quad , \tag{4a}$$

$$D_{\sigma p}(m,y) = \frac{\sigma_p(m,y) - \sigma_p(m)}{\sigma_{\sigma p}(m)} \quad . \tag{4b}$$

For each month we thus have two dimensionless deviations, D_{rp} and $D_{\sigma p}$, for the three presumably most important weather parameters p. The largest absolute value of these 6 deviations is now used to rank the month according to how "typical" its means and variations are. That is, for each calendar month, the months in the multi-year record are ranked according to increasing value of the largest absolute deviation.

Among the three top ranked months (i.e. the months with lowest maximum deviation), the highest ranked month devoid of "abnormal" weather conditions is finally elected as the "best" month. "Abnormal" weather here means that some relevant weather parameter, beyond the above three, has a monthly average that deviates more than one standard deviation (3b) from the multi-year calendar month average (3a) or, preferably, from the standard normal (30 years) monthly average.

3.2 The adjustment process

Next, the "best" months get frequency distributions for the most important weather parameters that equal the distributions seen within the respective calendar month's multi-year record. For example, each hourly temperature x in the "best" month is adjusted to a new temperature y, so that the percentage of hourly temperatures less than x in the "best" month equals the percentage of hourly temperatures less than y in the calendar month's multi-year record. For example, the median hourly value in the "best" month is not moved in time, but merely replaced by the median hourly value in the multi-year record.

This adjustment is applied to dry bulb temperature, wind speed and normal beam irradiance, while adjusted global irradiance is calculated from adjusted normal beam and unadjusted diffuse irradiance. Adjusted dewpoint temperatures are calculated from adjusted dry bulb temperatures and unadjusted relative humidities. Finally, jumps in temperatures and wind speed by change from one month to the next are smoothed over 6 night hours.

Whenever the unadjusted "best" month has a greater percentage of hours with no beam irradiance than has the corresponding multi-year record, an ambiguity arises with respect to which of these hours should be given some beam irradiance. To avoid foolish upward adjustments in such cases (e.g. at night-time), a sufficient number of overcast hours around mid-day and mid-month in the unadjusted "best" month are pre-elected as candidates. These candidate hours are flagged simply by giving them different negligibly small beam irradiances. If needed, the adjustment process then selects them in descending order and gives them the smallest beam irradiances of the adjusted final month. If the number of flags is too large, the remaining flag irradiances are adjusted back to zero.

Note that the rank numbers of the hourly weather parameters are not changed during the above process. For example, if the twelfth hour of the seventeenth day happens to have the twentythird highest temperature in the unadjusted "best" month, it will have so even in the adjusted "best" month. Therefore, the adjustment does not appreciably change the auto-/crosscorrelation structure of the unadjusted "best" month. That is, while the adjustment always yields frequency distributions in full accordance with the multi-year distributions, the final auto-/crosscorrelation structure depends entirely on the selection of a "best" month having a representative correlation structure from the outset. One assumption underlying the "Danish" selection method, is exactly that such representativeness is obtained by searching the multi-year record for the "most typical" monthly averages and variations of the three most important weather parameters.

3.3 The reconstruction process

As an example, Table 1 lists the weather parameters included in the DRYs produced for Bergen and Oslo, Norway. The paucity of complete historic records of all these weather parameters frequently hampers DRY production. While well-known interpolation schemes can make up for short data gaps, the complete lack of data may be the case for some weather parameters. In particular, the latter applies to radiation data, and models are therefore frequently used to derive missing data. The kind of models involved are reviewed in [19-24], and the models used in the production of the Norwegian DRYs are outlined as examples below.

3.3.1 GLOBAL IRRADIANCE

Several empirical relations between cloudiness and global irradiation are published in the past, e.g. in [19,22,25,26]. Since monthly average cloud data are far more abundant than are global radiation data, the monthly relations may be used to produce maps (Fig. 5) of mean monthly global irradiation [27,28,29]. Moreover, as exemplified in Fig. 6 [11], monthly global irradiations are readily transformed to frequency distributions of hourly global irradiation. Such distributions are useful for many purposes, but it takes a lot of doing to "edit" them into records of hourly weather data in a way that produces a representative auto-/crosscorrelation structure.

However, routine observations of cloud amount and type, available on an hourly basis from a number of airports, provide sufficient input to model hourly global irradiances with key statistical properties very close to those of observed data. For example, applied to independent data, the model [13] yields mean bias errors less than 3%, and frequency distributions close to the observed ones (Fig. 7). The observed overall lag one autocorrelation coefficients were 0.87 and 0.63-0.66

Table 1. Design Reference Year format: Data, with Format and Columns, are for each Parameter given hourly (h) or at Frequencies specified in CET. Radiation data are hourly integrals with beginning/end specified by parameter 2. Parameter 35 is an estimated maximum for each hour. Total cloud amount, either observed (12) or modified by halving high clouds (13), are given on a common scale 0-80 for observations recorded in oktas or tenths. The optional data 18-29 are those given for Bergen and Oslo, but even static stability or forecasts may be given here, if available.

Par		Freq	Form	Col
	Record 1			
1	Station identification	h	I5	1-5
2	Time index for radiation data	h	A1	6
3	Dry bulb temperature (2 m), 0.1°C	h	I4	7-10
4	Dew point temperature (2 m), 0.1°C	h	I4	11-14
5-7	Global/diffuse/normal beam irradiance, Wm^{-2}	h	3I4	15-18
8	Longwave atmospheric irradiance, Wm^{-2}	h	I4	27-30
9-11	Global/diffuse/normal beam illuminance, lux	h	3I5	31-45
12	Concurrent total cloud amount, 0-80	h	I2	46-47
13	Equivalent opaque cloud amount, 0-80	h	I2	48-49
14	Sunshine duration, minutes	h	I3	50-52
15	Wind direction 10 m, last 10 min, deca degrees	h	I2	53-54
16	Wind speed 10 m, last 10 min, 0.1 ms^{-1}	h	I3	55-57
17	Index for optional data (18-29) to follow:	h	I2	58-59
18	Max. temperature last 12 hours, 0.1°C	7&19	I4	60-63
19	Min. temperature last 12 hours, 0.1°C	7&19	I4	64-67
20	Concurrent station pressure, hPa	h	I4	68-71
21	Precipitation last 12 hours, mm	7&19	I4	72-75
22	Concurrent weather, WMO code 0-99	h	I2	76-77
23	Past weather (since last observation), — " —	h	I2	78-79
24	Snow cover at 7h CET, 0-4	7	I2	80-81
25-29	Empty		10X	82-91
30-32	Year, month, date	h	3I2	92-97
33	Hour, local standard time, 01-24	h	I2	98-99
34	Continuation mark, 0 or 1	h	I1	100
	Record 2 (only if Continuation mark = 1)			
35	Maximum hourly normal beam irradiance, Wm^{-2}	h	I5,1X	1-6
36-47	Sequence of 5 min normal beam irradiance, in % of 35	h	12I3	7-42
48-50	Month, date, hour	h	1X,3I2	43-49
51	Continuation mark (here always 0)	h	I1	50

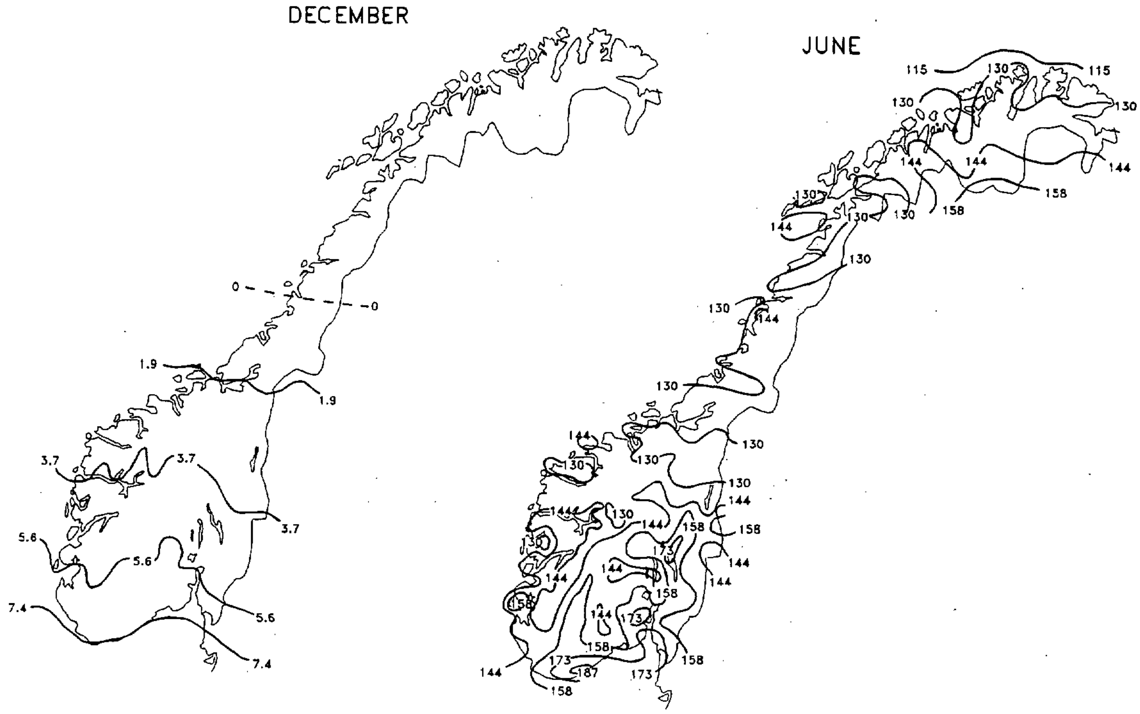

Fig.5 Isolines (Wm^{-2}) for mean global irradiance derived from mean cloud cover [27,28,29].

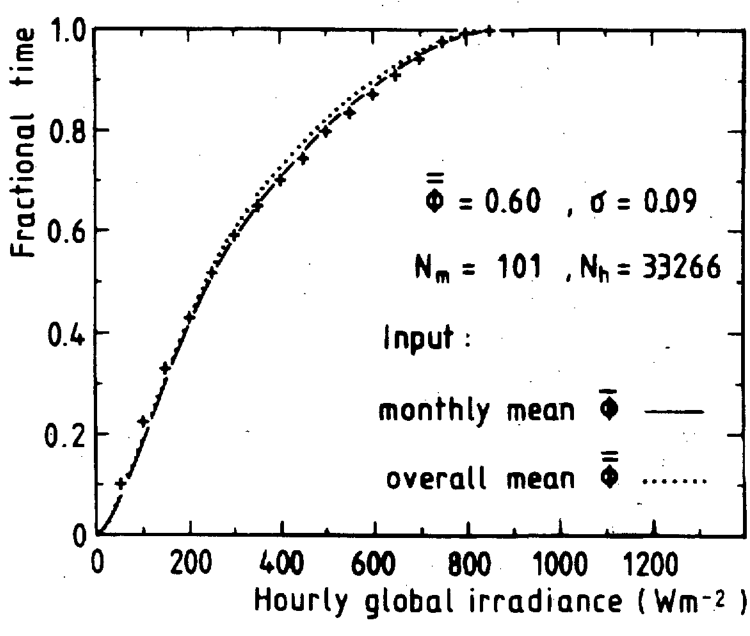

Fig.6 Fractional time distributions of hourly global irradiance at Ås (1968-79): Observed (+), modelled from individual monthly averages (full line), and modelled from the overall 12 year average (dotted line) [11].

for, respectively, hourly and daily global irradiation. This is close to the corresponding coefficients from modelled data, viz. 0.89 and 0.65-0.70. Removing the solar elevation influence by forming normalized clearness indices, yields observed lag one autocorrelations 0.87-0.88 and 0.36-0.41 for, respectively, hourly and daily data, pretty close to the corresponding coefficients from modelled data, viz. 0.90-0.93 and 0.34-0.45. Moreover, since the model explicitly accounts for cloudiness and solar elevation, with their crosscorrelations to other weather parameters, even the observed crosscorrelations are realistically reproduced.

On the contrary, if cloud observations are the missing ones, values should be estimated from global radiation or from sunshine duration, at least for solar zenith angles $< 80°$. Such computed cloud amounts, obtained e.g. by inverting relations given in [13], will be strongly related to the cloud conditions in the vicinity of the sun's angular position. This is acceptable because the accuracy demands are normally low for cloud data used in various application programmes, e.g. for the distribution of diffuse irradiance from the sky. However, due to the generally marked diurnal variation in cloud amount, such estimated daytime cloud amounts are not recommended for the estimation of longwave radiative cooling during the previous or subsequent night (see chap. 3.3.5.).

3.3.2 Slope irradiance

Available solar radiation records are generally of global radiation, while data requests from the solar energy community frequently refer to sloping planes. The division of a DRY's global radiation, into its beam and diffuse components, is therefore required to facilitate derivation of requested data.

Due to strong non-linearities, empirical models for the diffuse fraction of monthly global radiation can generally not be used with hourly data, even though these monthly models are in nice accordance with their hourly counterparts [11]. Moreover, in particular if vertical sun facing slopes and low solar elevations are involved, it is important to interpret extremely high global irradiances, whether real or spurious, as derived from extremely high diffuse irradiances rather than from beam irradiances exceeding realistic upper limits. The model [30], expressing the hourly diffuse fraction of global irradiance in terms of hourly solar elevation and clearness index (Fig. 8), explicitly meets this latter requirement and it also fairly well fits the average picture of an extensive independent data base. Note, however, that including even the interhour variability of global irradiance as input, further improves the performance of such empirical models [31]. Given a correct division of global irradiance into its beam and diffuse components, the beam irradiance on a given slope is readily computed. To calculate the diffuse slope irradiance requires additional information about surface reflectance and the angular distribution of sky radiance.

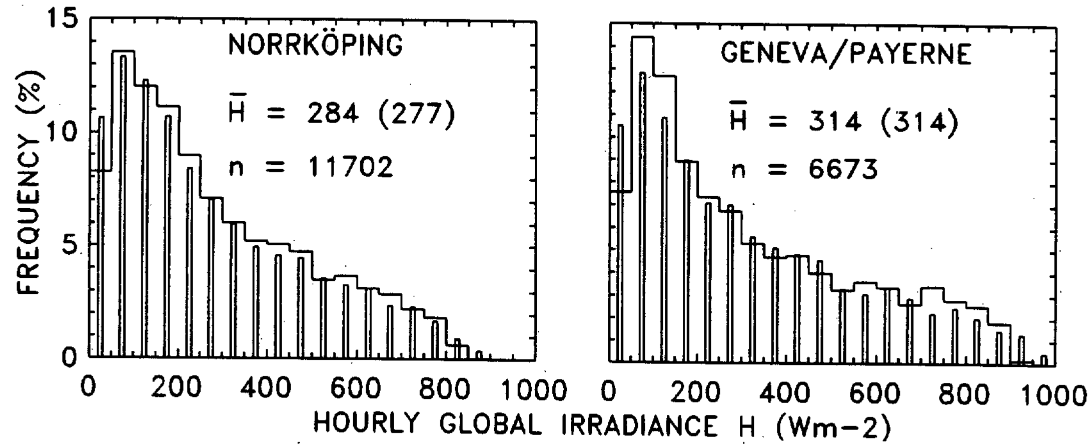

Fig.7 Overall distributions of observed hourly global irradiance (histograms), and corresponding distributions (bars) modelled from hourly cloud data. Observed mean values H are given with the corresponding modelled values in parenthesis, and n = number of hours [13].

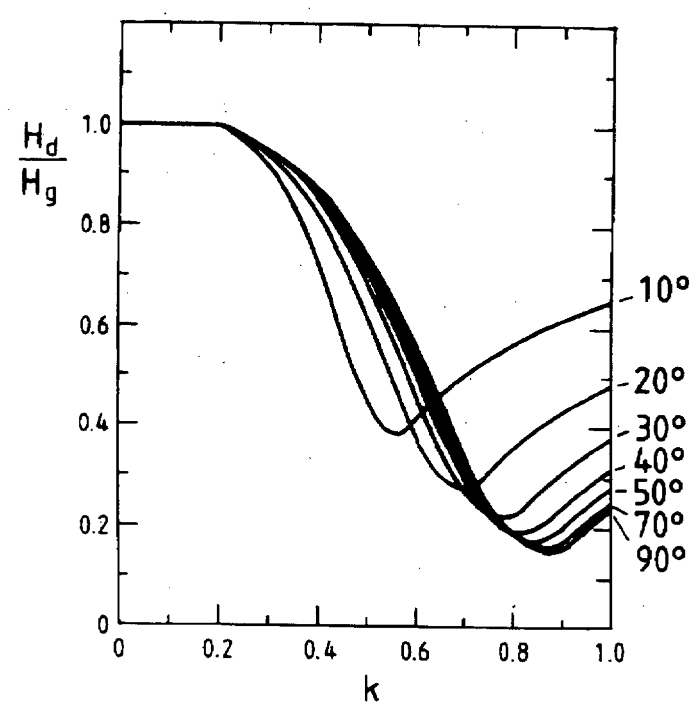

Fig.8 Modelled hourly diffuse fraction H_d/H_g as a function of clearness index k (surface global radiation : extraterrestrial global radiation) for various solar elevations [30].

The hourly model [32], assumes Lambertian ground reflectance and accounts for local horizon effects. Sky radiance anisotropy for cloudless as well as overcast skies is parameterized as follows: One fraction, equal to the beam transmittance, of the horizontal diffuse irradiance is treated as circumsolar radiation [33]. Another fraction, decreasing from 0.3 at overcast to zero at beam transmittance = 0.15, is treated as collimated radiation from the zenith. The remaining horizontal diffuse irradiance is treated as isotropic sky dome radiance.

Tested against 12 independent slope irradiance data sets, the model [32] ranked as number 5 of 21 models [20]. Applied on 5 different slopes at Bergen (Fig. 9), it yields hourly root-mean-square errors ranging from 14 Wm^{-2} on north vertical to 22 Wm^{-2} on south vertical. This amounts to, respectively, 5 and 2% of the corresponding observed ranges [34].

3.3.3 DAYLIGHT ILLUMINANCE

Most radiation-driven processes are spectrally selective, like the photosynthesis or the erythemal response of human skin to ultraviolet radiation. Equally well-known is the concept of daylight, i.e. solar radiation evaluated in proportion to its capability of stimulating the human eye. Even though daylight data are in great demand, they frequently have to be estimated from prescribed luminous efficacies and observed or estimated beam and diffuse irradiance.

The luminous efficacy model [35] is based on the CIE curve for photopic vision and spectral irradiances obtained by an interpolation between transmittance models for, respectively, cloudless sky [36] and unbroken cloud cover [37]. This interpolation decomposes the diffuse irradiance into "blue sky", "dark cloud", and "bright cloud" irradiance (Fig. 10). For partly cloudy cases the model was slightly tuned to hourly global illuminances and irradiances from Bergen. The parameterized version of the model requires solar elevation, day of year, and diffuse and beam clearness indices as input.

Tested against one year of independent 15 min data from Albany, New York [38], the model [35] reasonably well reproduces observed group mean luminous efficacies ranging from 55 to 175 lumen/W (Fig. 11). The most pronounced outliers are beam efficacies at low beam irradiance and diffuse efficacies at low solar elevation under cloudless sky [39,40], both negligibly affecting the overall performance of the model (Fig. 12). Thus, the frequency distributions of observed, respectively modelled diffuse and normal beam illuminances are almost identical, the mean bias errors are some 4% in both cases, and the correlation between observed and modelled values is 0.956 for diffuse and 0.996 for normal beam illuminance. Comparing observed global illuminances with those modelled from global irradiances (divided into beam and diffuse by the model [30]), shows close to identical distributions, mean bias error less than 2%, and a correlation coefficient 0.999 (Fig. 12).

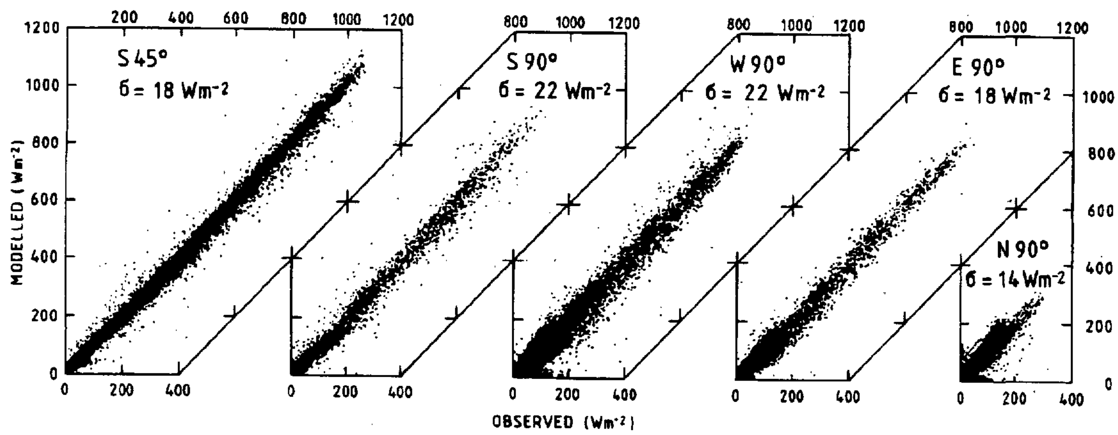

Fig.9 Modelled vs. observed hourly total solar irradiance on 5 slopes at Bergen (1978-83), together with the root-mean-square error σ [34].

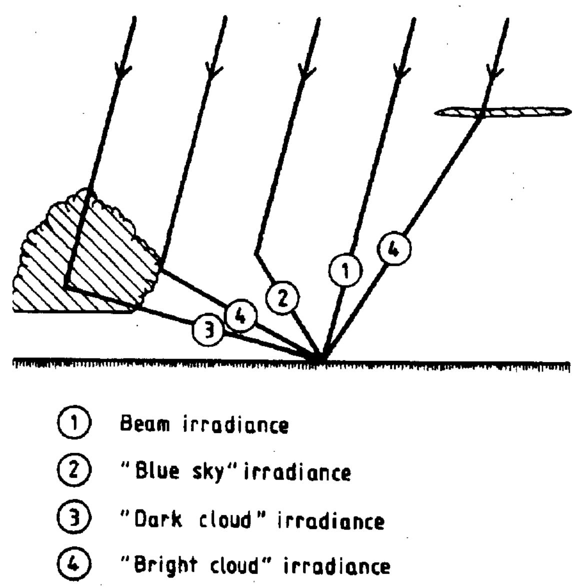

Fig.10 Schematic illustration indicating the four components into which the global irradiance is decomposed for luminous efficacy calculations [35].

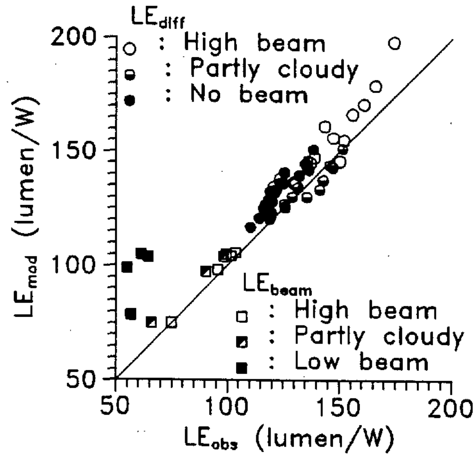

Fig.11 Modelled vs. observed group mean values of luminous efficacy, with the 1:1 line drawn for comparison. Data (15 min averages) are grouped according to solar elevation and the level of beam irradiance [39,40].

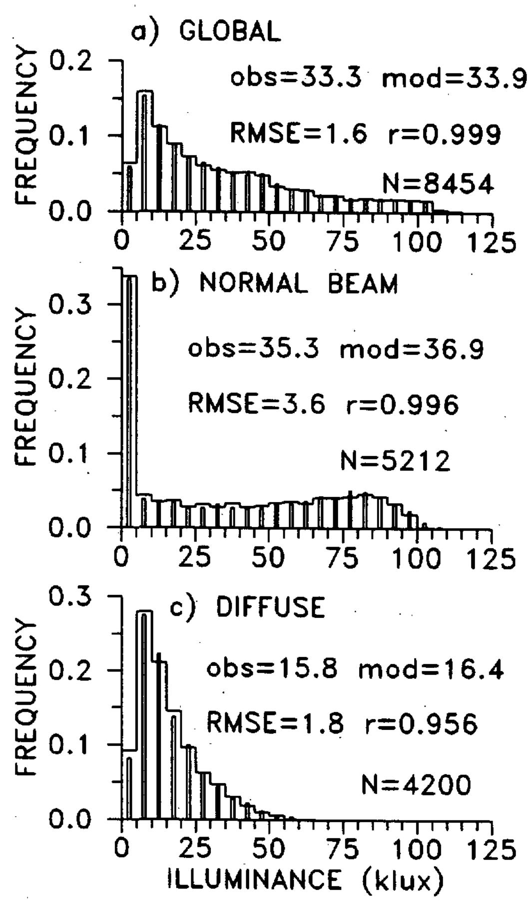

Fig.12 Observed (histograms) and modelled (bars) frequencies of 15 min global, normal beam, and diffuse illuminance. Observed (obs) and modelled (mod) averages, root-mean-square error RMSE, correlation coefficient r, and number N of 15 min values are given [39,40].

3.3.4 SHORT-TERM GLOBAL AND BEAM IRRADIANCE

Since clouds tend to give solar radiation an "on-off" character, hourly averages may imply far more smoothing in the case of solar irradiance than in the case of e.g. air temperature. Hourly irradiances are nevertheless sufficient for most applications. For active solar systems with lightweight absorbers and suitable control systems, however, increased efficiencies are measured and even simulated, during periods with short-term (minutes) solar irradiance variations.

Due to the widespread lack of recorded short-term irradiances, an empirical model was developed [12]. This model derives the probability density distributions of short-term (averaging time < 10 min) global and beam irradiances from averaging time and calculated cloudless, respectively observed hourly irradiances. A first order autoregressive model turns these distributions into sequences of beam and global irradiances.

It turned out (Fig. 13) that if a finer time resolution than 1 hour is required, significant information is gained by reducing the averaging time to 5 min, while only slight additional information is obtained by a further reduction [12]. Since the beam component is the most important for most applications, we therefore give 5 min modelled normal beam irradiances in our DRYs. The diffuse irradiance, being less critical in the present context, is considered constant through each hour.

3.3.5 LONGWAVE IRRADIANCE

To calculate how an object with given emissivity and temperature is cooled by exchanging longwave radiation with the sky dome, requires longwave irradiance data which are frequently not available. Longwave atmospheric irradiance on a horizontal surface is specified in our DRYs, and even longwave slope irradiance may be derived from these horizontal data [41,42].

Since most of the irradiance at the surface derives from the lowest 100 - 400 m of a cloudless atmosphere, the cloudless sky irradiance is fairly accurately parameterized in terms of surface air temperature, with surface humidity adding only minor additional information [43]. As an example, Fig. 14 [44] shows the nice conformity for 6 model atmospheres between the 2 cm^{-1} resolution band model MODTRAN [45] which requires profiles (0-100 km) of composition and temperature as input, and two all-wave models, where [43] requires only surface air temperature while [46] requires both air temperature and humidity as input.

In addition to the cloudless sky component, clouds contribute irradiance mainly within the "atmospheric window". At the surface this cloud contribution varies within the same approximate range (0 - 100 Wm^{-2}) as does the net longwave radiative loss from a horizontal surface at air temperature. Its variability, due to variations in cloud emissivity and temperature, and in the

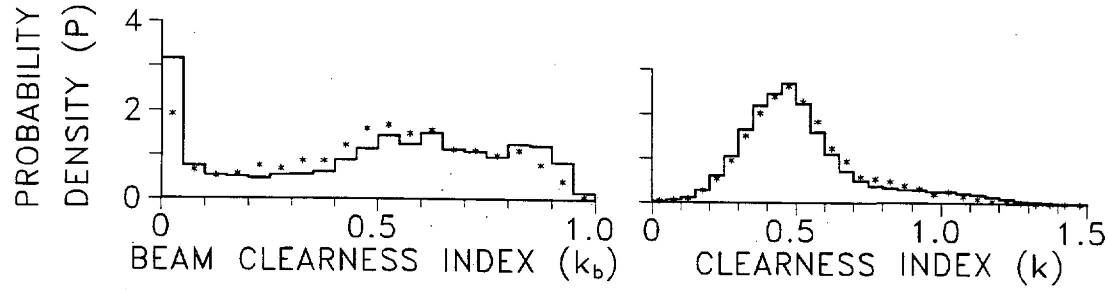

Fig.13 Observed distributions of instantaneous (histograms) and 5 min (*) averages of normalized global and beam clearness index. Data from Payerne, Switzerland for hours with average solar elevation > 15°, average clearness index within the interval 0.4 through 0.6 and high expected intrahour variability [12].

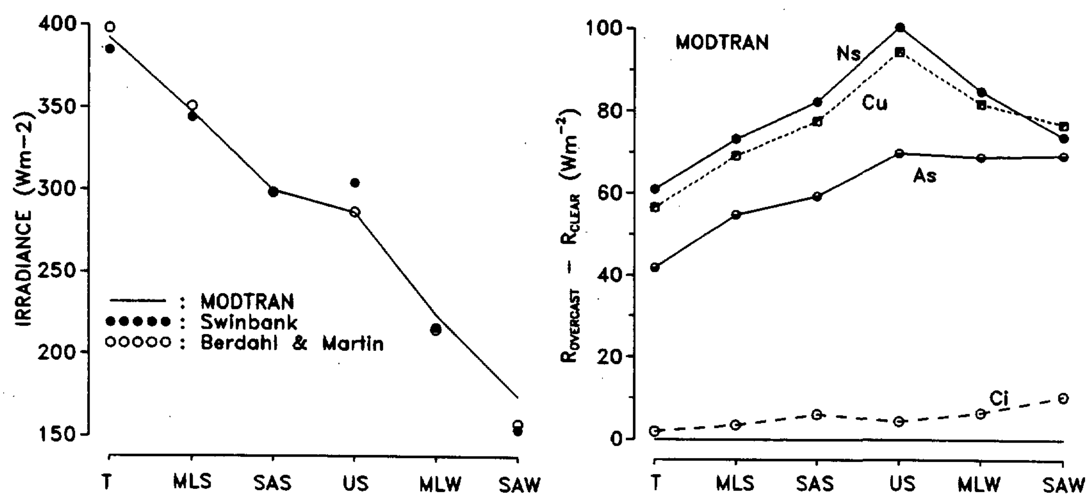

Fig.14 Left: Downwelling longwave irradiance at the surface calculated by three different models for 6 different cloudless atmospheres: Tropical, Mid Latitude Summer, Sub Arctic Summer, 1976 US Standard, Mid Latitude Winter, and Sub Arctic Winter.
Right: The increase of downwelling longwave irradiance at the surface calculated by MODTRAN for the 6 model atmospheres with 4 different cloud types: Nimbostratus, Cumulus, Altostratus, and Cirrus [44].

intervening atmosphere's transmittance, is exemplified by MODTRAN calculations for 4 cloud types in 6 model atmospheres (Fig. 14). Accurate cloud information is not readily inferred from surface data, and the cloud contribution is therefore modelled less exactly than the cloudless sky component.

3.3.6 FORECASTS

Some "intelligent" energy management systems can store energy, in the building fabric or in separate storages, for later usage. The purpose can be to utilize cheap off-peak electricity rates, to obtain a peak-shaving effect, or to obtain maximum peak hours electric output in cogeneration systems. Such systems need meteorological forecasts for 6-72 hours together with concurrent data.

To facilitate the simulation of such intelligent systems, the DRY should include forecasts. They should be given in the same numerical form and at the same hours as the Weather Services deliver them today. They should contain dry bulb temperature, wind speed, cloud amount, and (if air conditioning is common) a humidity parameter.

Since the format and time horizon of forecasts have changed much in recent years, it has proved difficult to get older forecasts in a homogenous format to be included in the DRY. One possibility is then to ask an experienced meteorologist to reconstruct (hindcast) the missing forecasts in todays format. Alternatively, if todays distribution of forecast errors are known, one can add errors drawn from that distribution to the known outcome, and use the sum as a reconstructed forecast.

4. REFERENCES

[1] Test Reference Year (TRY). Final Report NATO/CCMS. Rational Use of Energy Pilot Study, Subproject Climatic Conditions and Reference Year. Report NATO/CCMS 60. August 1977. Office Conservation, ERDA.

[2] H. LUND (1991): The Design Reference Years. In Buildings Simulation '91, 2nd World Congress on Technology improving the Energy Use, Comfort and Economics of Buildings Worldwide, Sophia Antipolis, Nice, France. August 20-22 1991.

[3] H. LUND & S. EIDORFF (1980): Selection methods for Production of Test Reference Years. Final report (short version), contract no. 284-77 ES DK, Report EUR 7306 EN.

[4] H. LUND (1985): Short Reference Years and Test Reference Years for EEC Countries. Thermal Insulation Laboratory, Technical University of Denmark. Final report, contract ESF-029-DK, Report EUR 10208 EN.

[5] M.A.M. SHALTOUT & M.T.Y. TADROS (1990): Test Reference Year for Cairo. Pp. 3035-3039 in Proc. 1st World Renewable Congress, UK, 23-28 September 1990, Pergamon Press 1990.

[6] I.J. HALL, R.R. PRAIRIE, H.E. ANDERSON & E.C.BOES (1978): Generation of a Typical Meteorological Year. Pp. 669-671 in Proc. of the 1978 Annual Meeting of the American Section of the International Solar Energy Society, Denver, Colorado.

[7] I.J. HALL, R.R. PRAIRIE, H.E. ANDERSON & E.C.BOES (1978): Generation of a Typical Meteorological Year for 26 SOLMET stations. Technical Report, Albuquerque, New Mexico.

[8] D.L. SIURNA, L.J. D'ANDREA & K.G.T. HOLLANDS (1984): A Canadian Representative Meteorological Year for Solar System Simulation. Pp. 85-88 in Proc. of the Tenth Annual National Meeting of Solar Energy Society of Canada, Calgary, Alberta.

[9] D.PISSIMANIS, G.KARRAS, V.NOTARIDOU & K.GAVRA (1988): The generation of a "Typical Meteorological Year" for the city of Athens. Solar Energy **40**, 405-411.

[10] J.A. OLSETH & A. SKARTVEIT (1984): A probability density function for daily insolation within the temperate storm belts. Solar Energy **33**, 533-542.

[11] J.A. OLSETH & A. SKARTVEIT (1987): A probability density model for hourly irradiance on arbitrarily orientated planes. Solar Energy **39**, 343-351.

[12] A. SKARTVEIT & J.A. OLSETH (1992): The probability density and autocorrelation of short-term global and beam irradiance. Solar Energy, **49**, 477-487.

[13] J.A. OLSETH & A. SKARTVEIT (1993): Characteristics of hourly global irradiance modelled from cloud data. Solar Energy, **51**, 197-204.

[14] J.A. OLSETH (1981): The solar radiation climate at Bergen (in Norwegian). Klima, No.4. The Norwegian Meteorological Institute, Oslo.

[15] J.A. OLSETH & K. HEGG (1982): A comparison of the solar radiation climate of Ås and Bergen (in Norwegian). Contributions from Agricultural University of Norway, Vol. 61, No. 16, 23 pp.

[16] R. FESTA & C.F. RATTO (1993): Proposal of a numerical procedure to select reference years. Solar Energy, **50**, 9-17.

[17] H. SAITO & Y. MATSUO (1974): Standard weather data for SHASE computer program of annual energy requirements and example results of hourly load for ten years in Tokyo. Second Symposium on the Use of Computers for Environmental Engineering related to Buildings, Paris, June 1974.

[18] R. DOGNIAUX & R. SNEYERS (1977): Méthodologie d'analyse statistique des données météorologiques en vu de la constitution de "periodes-types" pour l'application a des problemes spécifiques. Institut Royal Météorologique de Belgique, 1977.

[19] J.A. DAVIES, D.C. MCKAY, G. LUCIANI & M. ABDEL-WAHAB (1988): Validation of models for estimating solar radiation on horizontal surfaces. Final Report IEA Task IX, Atmospheric Environment Service, Ontario, Canada.

[20] J.E. HAY & D.C. MCKAY (1988): Calculation of solar irradiances for inclined surfaces: Verification of models which use hourly and daily data. Final Report IEA Task IX. Atmospheric Environment Service, Ontario, Canada.

[21] A.J. ARNFIELD (1979): Evaluation of empirical expressions for the estimation of hourly and daily totals of atmospheric longwave emission under all sky conditions. Quart. J. R. Met. Soc. **105**, 1041-1052.

[22] F. KASTEN, H.J. GOLCHERT & M. STOLLEY (1983): Parameterization of radiation fluxes as function of solar elevation, cloudiness, and turbidity. In Solar Energy R&D in the European Community, Series F, Vol. **2**.

[23] R. PEREZ, P. INEICHEN, R. SEALS, J. MICHALSKY & R.STEWART (1990): Models that use global and direct irradiance as input to predict other irradiance and daylight availability quantities. Solar Energy **44**, 271-289.

[24] R. FESTA & C.F. RATTO (1991): Report on Solar Radiation Statistical Properties. 277 pp. To be published.

[25] E.L. MAXWELL, L. ISMAILIDAS & N. DOESKEN (1989): Impact of cloud climates on solar radiation resources. SOLAR 89, Proc. Amer. Solar Energy Soc. (1989) 483-488.

[26] J.A DAVIES & D.C. MCKAY (1988): Estimating solar radiation from incomplete cloud data. Solar Energy **41**, 15-18.

[27] A. GULBRANDSEN & P.O. TANGEN (1977): Solar radiation in Norway (in Norwegian). University of Bergen.

[28] J.A. OLSETH & A.SKARTVEIT (1985): Radiation Handbook (in Norwegian). Klima, No. 7. The Norwegian Meteorological Institute, Oslo.

[29] J.A. OLSETH & A. SKARTVEIT (1986): The solar radiation climate of Norway. Solar Energy **37**, 423-428.

[30] A. SKARTVEIT & J.A. OLSETH (1987): A model for the diffuse fraction of hourly global radiation. Solar Energy **38**, 271-274.

[31] R. PEREZ, P. INEICHEN, R. SEALS & A. ZELENKA (1990): Making full use of the clearness index for parameterizing hourly insolation conditions. Solar Energy **45**, 111-114.

[32] A. SKARTVEIT & J.A. OLSETH (1986): Modelling slope irradiance at high latitudes. Solar Energy **36**, 333-344.

[33] J.E. HAY (1979): Study of shortwave radiation on non-horizontal surfaces. Report No 79-12, Atmospheric Environment Service, Downsview, Ontario.

[34] J.A. OLSETH & A. SKARTVEIT (1989): Radiation data, methods of calculation and presentation for Nordic conditions (in Norwegian). Nordic Solar Energy Days, Trondheim, Norway, 24-25 May 1989.

[35] J.A. OLSETH & A. SKARTVEIT (1989): Observed and modelled luminous efficacies under arbitrary cloudiness. Solar Energy **42**, 221-233.

[36] R.E. BIRD & C. RIORDAN (1986): Simple solar spectral model for direct and diffuse irradiance on horizontal and tilted planes at the earth's surface for cloudless atmospheres. J. Climate Appl. Meteor. **25**, 87.

[37] G.L. STEPHENS, S. ACKERMAN & E.A. SMITH (1984): A short-wave parameterization revised to improve cloud absorption. J. Atmos. Sci. **41**, 687.

[38] R. PEREZ (1991): One year of data from Albany, New York (personal communication).

[39] J.A. OLSETH & A. SKARTVEIT (1993): Modelling daylight illuminance and photosynthetic active irradiance. Proceedings of ISES World Congress 1993, Budapest, Hungary, 143-148.

[40] A. SKARTVEIT & J.A. OLSETH (1994): Luminous efficacy models and their application for calculation of photosynthetically active radiation. Solar Energy (in press).

[41] M.H. UNSWORTH & J.L. MONTEITH (1975): Longwave radiation at the ground. Quart. J. R. Met. Soc. **101**, 13-34.

[42] R.J. COLE (1979): The longwave radiation incident upon inclined surfaces. Solar Energy **22**, 459-462.

[43] W.C. SWINBANK (1963): Longwave radiation from clear skies. Quart. J. R. Met. Soc. **89**, 339-348.

[44] J.A. OLSETH & A. SKARTVEIT (1994): A comparison between longwave atmospheric irradiance formulae and MODTRAN over a wide range of climates (third draft). IEA-SHCP Task 17, Expert Meeting, Saratoga Springs, NY, USA, 9-11 March 1994.

[45] F.X. KNEIZYS, E.P. SHETTLE, L.W. ABREU, J.H. CHETWYND, G.P. ANDERSON, W.O. GALLERY, J.E.A. SELBY & S.A. CLOUGH (1988): Users Guide to LOWTRAN7, AFGL-TR-88-0177, Air Force Geophysics Laboratory, Hanscom AFB, MA 01731.

[46] P. BERDAHL & M. MARTIN (1984): Emissivity of clear skies. Solar Energy **32**, 663-664.